# Optimizing Parameters for Static Equilibrium of Discrete Elastic Rods with Active-Set Cholesky Supplementary Material

Tetsuya Takahashi and Christopher Batty

# I. 2D AND 4D CURVATURES

Figure 1 shows the strand configuration to illustrate the curvatures in the Discrete Elastic Rod (DER) formulation [1, 2]. Given the two incident edges and two material frames incident on a vertex, the associated 4D per-vertex material curvature degrees of freedom  $\kappa_i = (\kappa_{i,0}, \kappa_{i,1}, \kappa_{i,2}, \kappa_{i,3})^T$  are defined in [1] (see Equation 2) as

$$\boldsymbol{\kappa}_{i,0} = (\kappa \mathbf{b})_i^T \mathbf{d}_2^{i-1},\tag{1}$$

$$\boldsymbol{\kappa}_{i,1} = -(\kappa \mathbf{b})_i^T \mathbf{d}_1^{i-1},\tag{2}$$

$$\boldsymbol{\kappa}_{i,2} = (\kappa \mathbf{b})_i^T \mathbf{d}_2^i, \tag{3}$$

$$\boldsymbol{\kappa}_{i,3} = -(\kappa \mathbf{b})_i^T \mathbf{d}_1^i, \tag{4}$$

where  $(\kappa \mathbf{b})_i$  denotes the curvature binormal on vertex i [1, 2],  $\mathbf{d}_1^i$  and  $\mathbf{d}_2^i$  are the first and second material frame (director) vectors on edge i, respectively. Thus, we can interpret these 4D curvature values  $\kappa_i$  as the per-vertex binormal curvature  $(\kappa \mathbf{b})_i$  evaluated on the four material frame vectors  $(\mathbf{d}_1^{i-1}, \mathbf{d}_2^{i-1}, \mathbf{d}_1^i, \mathbf{d}_2^i)$ . By contrast, 2D curvatures  $\kappa_i = (\kappa_{i,0}, \kappa_{i,1})^T$  are defined in [2] (see the equation preceding Section 3.2) as

$$\boldsymbol{\kappa}_{i,0} = (\kappa \mathbf{b})_i^T \frac{\mathbf{d}_2^{i-1} + \mathbf{d}_2^i}{2},\tag{5}$$

$$\boldsymbol{\kappa}_{i,1} = -(\kappa \mathbf{b})_i^T \frac{\mathbf{d}_1^{i-1} + \mathbf{d}_1^i}{2}.$$
 (6)

This computation can be interpreted as the binormal curvature  $(\kappa \mathbf{b})_i$  evaluated on the *averaged* material frames  $\left(\frac{\mathbf{d}_1^{i-1}+\mathbf{d}_1^i}{2},\frac{\mathbf{d}_2^{i-1}+\mathbf{d}_2^i}{2}\right)$  at the vertex. As the averaged material frames can be non-unit and non-orthogonal (e.g., when the strand is twisted or flipped), the 2D curvatures [2] can fail to correctly reflect the true curvatures of the strand.

# II. GRADIENTS

In the following, we provide details on the gradient of the objectives in DER.

#### A. Inertia

The gradient of the inertia objective is given by

$$\nabla E_{\rm in}(\mathbf{q}) = \frac{\mathbf{M}}{\Delta t^2} (\mathbf{q} - \mathbf{q}^*). \tag{7}$$

Tetsuya Takahashi is with Tencent America, USA; Christopher Batty is with University of Waterloo, Canada

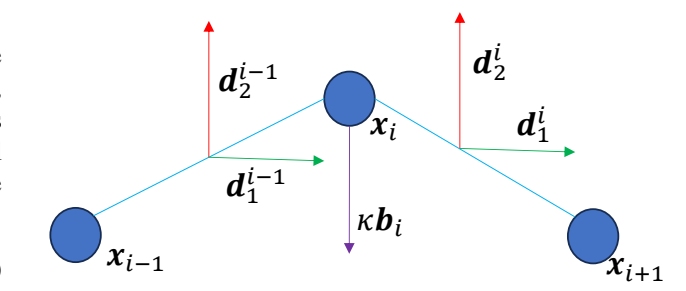


Fig. 1. Strand configuration for illustrating curvatures with three vertices (blue circles) with positions  $\mathbf{x}_{i-1}$ ,  $\mathbf{x}_i$ ,  $\mathbf{x}_{i+1}$  and two edges (cyan lines). Green and red arrows represent material frames on the edges  $(\mathbf{d}_1^{i-1}, \mathbf{d}_2^{i-1}, \mathbf{d}_1^i, \mathbf{d}_2^i)$ . The purple arrow represents the curvature binormal  $(\kappa \mathbf{b})_i$ .

# B. Stretching

The gradient of the stretching objective on edge i is given by

$$\nabla_{\mathbf{x}_{i+1}} E_{\mathrm{st},i}(\mathbf{x}_i, \mathbf{x}_{i+1}) = -\nabla_{\mathbf{x}_i} E_{\mathrm{st},i}(\mathbf{x}_i, \mathbf{x}_{i+1})$$
(8)

$$= s\alpha_i \pi r^2 (\mathbf{l}_i \overline{\mathbf{l}}_i^{-1} - 1) \mathbf{t}_i, \qquad (9)$$

where  $\mathbf{t}_i = \frac{\mathbf{x}_{i+1} - \mathbf{x}_i}{\mathbf{l}_i}$  denotes the unit tangent vector of edge i.

# C. Bending

The 11-dimensional gradient of the bending objective on vertex i [3] is given by

$$\nabla E_{\mathrm{be},i}(\mathbf{y}_i) = \left(\frac{s\boldsymbol{\beta}_i \pi r^4}{4(\bar{\mathbf{l}}_{i-1} + \bar{\mathbf{l}}_i)}\right) \mathbf{J}_{\mathrm{cu},i}^T(\boldsymbol{\kappa}_i - \bar{\boldsymbol{\kappa}}_i), \tag{10}$$

where  $\mathbf{J}_{\mathrm{cu},i} \in \mathbb{R}^{4 \times 11}$  denotes the Jacobian of  $\boldsymbol{\kappa}_i$  with respect to  $\mathbf{y}_i$ . Here,  $\mathbf{J}_{\mathrm{cu},i}^T(\boldsymbol{\kappa}_i - \bar{\boldsymbol{\kappa}}_i) = \sum_{j=0}^3 (\boldsymbol{\kappa}_{i,j} - \bar{\boldsymbol{\kappa}}_{i,j}) \nabla \boldsymbol{\kappa}_{i,j}$ , where  $\boldsymbol{\kappa}_{i,j}$  denotes the jth entry of  $\boldsymbol{\kappa}_i$  [4, 5].

#### D. Bending

The 11-dimensional gradient of the twisting objective is given by

$$\nabla E_{\text{tw},i}(\mathbf{y}_i) = \left(\frac{s\boldsymbol{\gamma}_i \pi r^4}{(\overline{\mathbf{I}}_{i-1} + \overline{\mathbf{I}}_i)}\right) (\mathbf{m}_i - \overline{\mathbf{m}}_i) \nabla \mathbf{m}_i.$$
(11)

#### III. FORCES AND JACOBIANS

We provide details on the forces and Jacobians.

#### A. Inertia

Given the inertia force defined as  $\mathbf{f}_{\rm in} = -\nabla E_{\rm in}(\mathbf{q})$  with  $\mathbf{q} = \mathbf{q}^t$  and  $\dot{\mathbf{q}}^t = 0$  for a static equilibrium case, we have  $\mathbf{f}_{\rm in} = \mathbf{f}_{\rm ext}$  and thus  $\frac{\partial \mathbf{f}_{\rm in}}{\partial \mathbf{p}} = 0$  [3].

# B. Stretching

We define the stretching force of edge i on vertex i+1 as  $\mathbf{f}_{\mathrm{st,i,i+1}} = -\nabla_{\mathbf{x}_{i+1}} E_{\mathrm{st,i}}(\mathbf{x}_i,\mathbf{x}_{i+1})$  (9), and define  $\mathbf{f}_{\mathrm{st,i,i}}$  analogously. Given the dependence of  $\mathbf{f}_{\mathrm{st,i,i+1}}$  and  $\mathbf{f}_{\mathrm{st,i,i}}$  on  $\overline{\mathbf{l}}_i$  and  $\alpha_i$ , their Jacobians are

$$\frac{\partial \mathbf{f}_{\mathrm{st,i,i+1}}}{\partial \bar{\mathbf{l}}_i} = -\frac{\partial \mathbf{f}_{\mathrm{st,i,i}}}{\partial \bar{\mathbf{l}}_i} = s\alpha_i \pi r^2 \mathbf{l}_i \bar{\mathbf{l}}_i^{-2} \mathbf{t}_i, \tag{12}$$

$$\frac{\partial \mathbf{f}_{\mathrm{st,i,i+1}}}{\partial \boldsymbol{\alpha}_i} = -\frac{\partial \mathbf{f}_{\mathrm{st,i,i}}}{\partial \boldsymbol{\alpha}_i} = -s\pi r^2 \left( \mathbf{l}_i \overline{\mathbf{l}}_i^{-1} - 1 \right) \mathbf{t}_i. \tag{13}$$

#### C. Bending

We define the bending force according to (10) by  $\mathbf{f}_{\mathrm{be},i} = -\nabla E_{\mathrm{be},i}(\mathbf{y}_i)$ . Given its dependence on  $\bar{\mathbf{I}}_{i-1}, \bar{\mathbf{I}}_i, \bar{\kappa}_{i,0}, \bar{\kappa}_{i,1}$ , and  $\boldsymbol{\beta}_i$  while respecting the constraints  $\bar{\kappa}_{i,0} = \bar{\kappa}_{i,2}$  and  $\bar{\kappa}_{i,1} = \bar{\kappa}_{i,3}$ , the Jacobians are given (with  $j \in \{0,1\}$ ) by

$$\frac{\partial \mathbf{f}_{\mathrm{be},i}}{\partial \bar{\mathbf{I}}_{i-1}} = \frac{\partial \mathbf{f}_{\mathrm{be},i}}{\partial \bar{\mathbf{I}}_{i}} = \left(\frac{s\boldsymbol{\beta}_{i}\pi r^{4}}{4(\bar{\mathbf{I}}_{i-1} + \bar{\mathbf{I}}_{i})^{2}}\right) \mathbf{J}_{\mathrm{cu},i}^{T}(\boldsymbol{\kappa}_{i} - \bar{\boldsymbol{\kappa}}_{i}), \quad (14)$$

$$\frac{\partial \mathbf{f}_{\mathrm{be},i}}{\partial \bar{\boldsymbol{\kappa}}_{i,j}} = \left(\frac{s\boldsymbol{\beta}_i \pi r^4}{4(\bar{\mathbf{I}}_{i-1} + \bar{\mathbf{I}}_i)}\right) (\nabla \boldsymbol{\kappa}_{i,j} + \nabla \boldsymbol{\kappa}_{i,j+2}),\tag{15}$$

$$\frac{\partial \mathbf{f}_{\mathrm{be},i}}{\partial \boldsymbol{\beta}_i} = -\left(\frac{s\pi r^4}{4(\overline{\mathbf{I}}_{i-1} + \overline{\mathbf{I}}_i)}\right) \mathbf{J}_{\mathrm{cu},i}^T(\boldsymbol{\kappa}_i - \overline{\boldsymbol{\kappa}}_i). \tag{16}$$

#### D. Twisting

We define the twisting force as  $\mathbf{f}_{\mathrm{tw},i} = -\nabla E_{\mathrm{tw},i}(\mathbf{y}_i)$  (11). Given its dependence on  $\bar{\mathbf{l}}_{i-1}, \bar{\mathbf{l}}_i, \ \bar{\mathbf{m}}_i$ , and  $\gamma_i$ , the Jacobians are given by

$$\frac{\partial \mathbf{f}_{\text{tw},i}}{\partial \overline{\mathbf{I}}_{i-1}} = \frac{\partial \mathbf{f}_{\text{tw},i}}{\partial \overline{\mathbf{I}}_{i}} = \left(\frac{s \boldsymbol{\gamma}_{i} \pi r^{4}}{(\overline{\mathbf{I}}_{i-1} + \overline{\mathbf{I}}_{i})^{2}}\right) (\mathbf{m}_{i} - \overline{\mathbf{m}}_{i}) \nabla \mathbf{m}_{i}, \quad (17)$$

$$\frac{\partial \mathbf{f}_{\text{tw},i}}{\partial \bar{\mathbf{m}}_i} = \left(\frac{s \gamma_i \pi r^4}{(\bar{\mathbf{l}}_{i-1} + \bar{\mathbf{l}}_i)}\right) \nabla \mathbf{m}_i,\tag{18}$$

$$\frac{\partial \mathbf{f}_{\text{tw},i}}{\partial \boldsymbol{\gamma}_i} = -\left(\frac{s\pi r^4}{(\overline{\mathbf{l}}_{i-1} + \overline{\mathbf{l}}_i)}\right) (\mathbf{m}_i - \overline{\mathbf{m}}_i) \nabla \mathbf{m}_i. \tag{19}$$

# IV. BENDING WITH 2D vs. 4D CURVATURES

We compare bending formulations using 2D and 4D curvatures to justify our choice of 4D curvatures, given that our parameter optimization includes only two rest curvatures per vertex. The analysis is conducted on a horizontal strand discretized with 30 vertices.

#### A. 2D Curvatures with Averaged Material Frames [2]

In Figure 2, we compare a bending model with 4D curvatures [1] against a bending model with 2D curvatures [2] which averages material frames to reduce curvature dimensions from 4D to 2D. We experiment with the horizontal strand without and with its material frames flipped, and use  $\mathbf{c}_{\mathrm{be}} = 10^{10}$ .

While both models without frame flips yield equivalent results, the 2D curvature model [2] fails to generate bending

forces when material frames are flipped because the averaged material frames can be non-unit vectors (in this example, averaged frames are zero vectors) [4]–[6]. By contrast, the 4D curvature model [1] correctly evaluates the bending even with the flipped frames, producing results consistent with those obtained without edge flips.

# B. 2D Curvatures with Spherically Interpolated Material Frames [6]

Figure 3 contrasts the bending model with 4D curvatures [1] against another model [6] with 2D curvatures, which spherically interpolates (i.e., uses slerp) material frames to maintain unit-size frames while reducing the curvature dimensions. We use flipped frames and  $\mathbf{c}_{\mathrm{be}} = 10^8, 10^9$ .

While the slerped material frames, which retain unit length, enable correct bending evaluation even with the flipped frames, differentiating the slerped frames to compute bending forces presents challenges. Consequently, their bending model [6] resorts to approximated gradients (which did not prove sufficiently accurate in our experiments) causing stability problems with the Gauss-Newton Hessian approximation. By contrast, the bending model of [1] is stable under the same settings.

#### V. COMPARISON WITH SINGLE STIFFNESS PARAMETER

In Figure 4, we evaluate the parameter optimization method with the bending stiffness defined per strand and per vertex, along with the naive initialization. In this evaluation, we use a horizontal strand discretized with 30 vertices and  $\mathbf{c}_{\mathrm{be}}=10^9$ . With the single parameter for the strand, we first optimize the material stiffness (so that rest shape optimization is sufficient to achieve static equilibrium) and then perform rest shape optimization [3].

With the single stiffness parameter for the strand, it is necessary to stiffen the entire strand and reach around  $4.5\times$  higher than the initial bending stiffness. Consequently, the generated behaviors of the strand appear stiffer than expected with the given initial stiffness. By contrast, our method stiffens only at the root end (reaching the  $4.5\times$  higher stiffness) to achieve static equilibrium and thus generates strand behaviors expected with the initially specified parameters at the tail end.

# REFERENCES

- M. Bergou, M. Wardetzky, S. Robinson, B. Audoly, and E. Grinspun, "Discrete elastic rods," in ACM SIGGRAPH 2008 Papers, ser. SIGGRAPH '08. New York, NY, USA: Association for Computing Machinery, 2008.
- [2] M. Bergou, B. Audoly, E. Vouga, M. Wardetzky, and E. Grinspun, "Discrete viscous threads," ACM Transactions on Graphics, vol. 29, no. 4, pp. 116:1–116:10, 2010.
- [3] T. Takahashi and C. Batty, "Rest shape optimization for sag-free discrete elastic rods," Computer Graphics Forum, vol. n/a, no. n/a, p. e70019.
- [4] J. Panetta, M. Konaković-Luković, F. Isvoranu, E. Bouleau, and M. Pauly, "X-shells: a new class of deployable beam structures," ACM Trans. Graph., vol. 38, no. 4, jul 2019.
- [5] Y. R. Fei, C. Batty, E. Grinspun, and C. Zheng, "A multi-scale model for coupling strands with shear-dependent liquid," ACM Trans. Graph., vol. 38, no. 6, Nov. 2019.
- [6] G. Gornowicz and S. Borac, "Efficient and stable approach to elasticity and collisions for hair animation," in *Proceedings of the 2015 Sympo*sium on Digital Production, ser. DigiPro '15. New York, NY, USA: Association for Computing Machinery, 2015, p. 41–49.

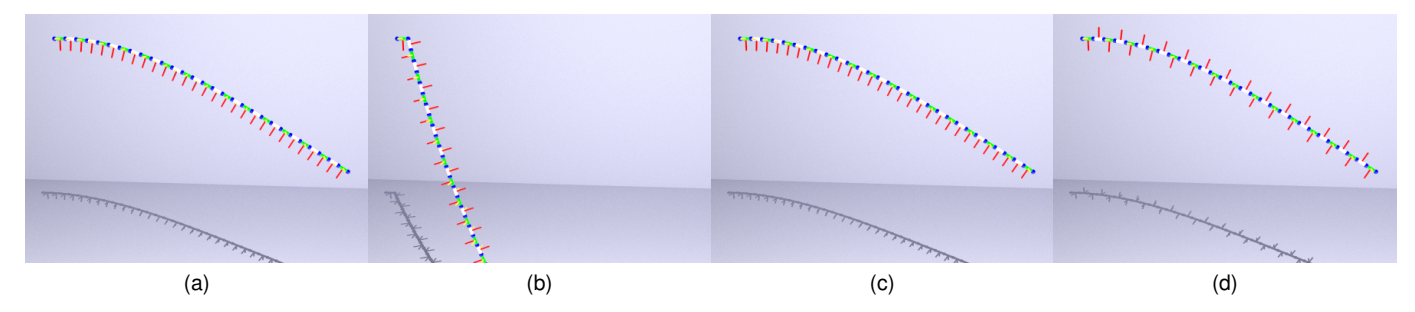


Fig. 2. Comparison of two bending models with a horizontal strand without and with flipped material frames. (a) 2D curvatures. (b) 2D curvatures with flipped frames. (c) 4D curvatures. (d) 4D curvatures with flipped frames. The bending model with 2D and 4D curvatures without frame flips can correctly evaluate bending and generate natural strand behaviors ((a) and (c)). With the flipped frames, the 2D curvature bending model fails to generate bending forces (b), whereas the 4D curvature bending model correctly handles the bending, generating the expected result (d).

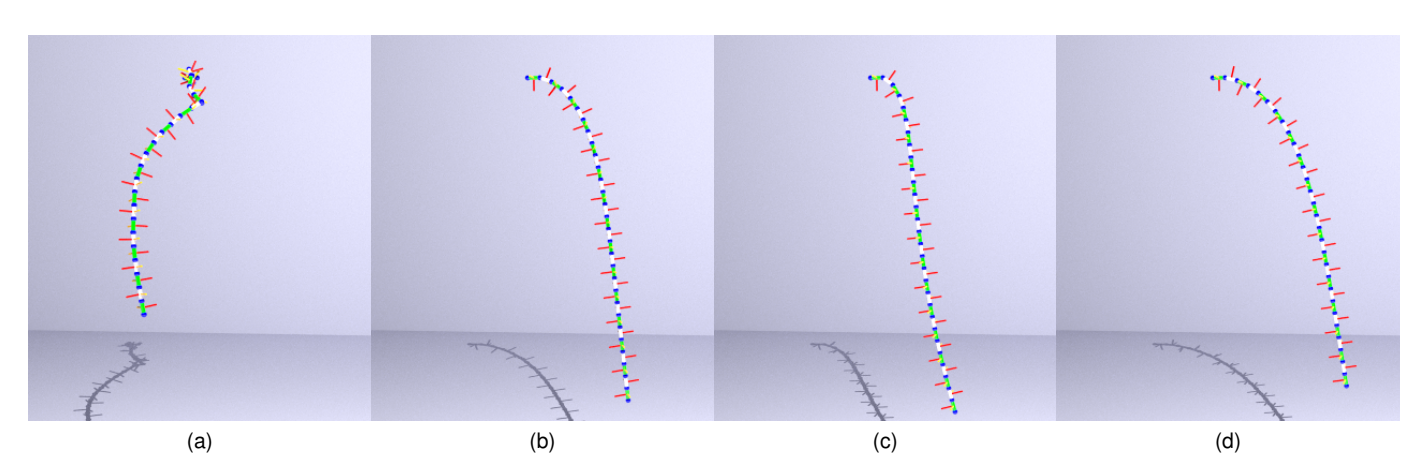
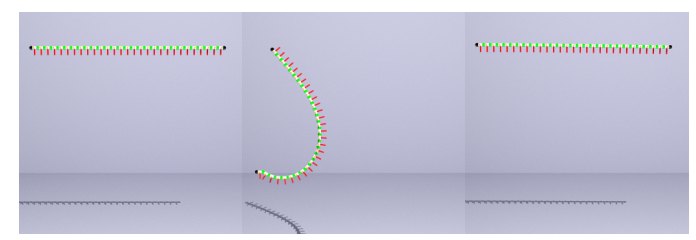


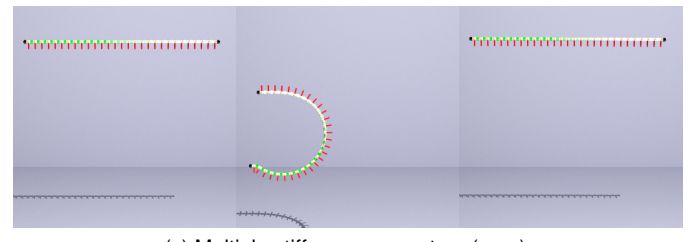
Fig. 3. Comparison of two bending models with a horizontal strand. 2D curvatures with slerp and  $\mathbf{c}_{\mathrm{be}}=10^8$  (a) and  $\mathbf{c}_{\mathrm{be}}=10^9$  (b). 4D curvatures with  $\mathbf{c}_{\mathrm{be}}=10^8$  (c) and  $\mathbf{c}_{\mathrm{be}}=10^9$  (d). While spherical interpolation enables correct evaluation of bending even with the flipped frames (b), approximated gradients can lead to stability problems (a). By contrast, the bending model with 4D curvatures generates natural strand behaviors ((c) and (d)).



# (a) Naive initialization



(b) Single stiffness parameter



(c) Multiple stiffness parameters (ours)

Fig. 4. A horizontal strand with its root perturbed vertically. White and green vertices represent low and high material stiffness for bending, while the black represents the undefined stiffness. The naive initialization fails to achieve static equilibrium while generating expected strand behaviors with the specified material stiffness (a). With a single stiffness parameter, while static equilibrium is achieved, the stiffness of the strand needs to be high for the tail end, giving the strand behaviors that appear stiffer than expected (b). Our method achieves static equilibrium while minimizing the stiffening of the strand and thus generating expected strand behaviors with the specified material stiffness (c).